The USE of INTERFEROMETRIC SAR for SURFACE RECONSTRUCTION

Bruno Crippa, Michele Crosetto, Luigi Mussio
DIIAR – Sez. Rilevamento - Politecnico di Milano
Piazza Leonardo da Vinci, 32 – 20133 MILANO – Italy
e-mail: bruno@ipmtf4.topo.polimi.it
miche — " —

Abstract

This paper presents the interferometric SAR (InSAR) procedure to generate Digital Elevation Models (DEMs) implemented at DIIAR - Polytechnic of Milan. The first part is concerned with the description of the complete InSAR procedure, giving particular emphasis to the original authors' contributions. The second part regards the analysis of the first results obtained processing a SAR data set covering South Catalunya (Spain).

Keywords: SAR Interferometry, DEM generation, DEM precision, Data fusion.

1. Introduction

The traditional use of SAR imagery in Remote Sensing is based on the amplitude of the radar signal; the images containing such amplitude are named classical SAR images. Since the late 1970s (Seasat mission) the space-borne classical SAR images have been used in a wide variety of application fields, including oceanography, geology, glaciology and land-use mapping.

In the last few years, a new and promising branch of the SAR technology based on the so-called complex SAR images has arisen. In such images, both the amplitude and the phase of the radar signal are available. When used in the interferometric way, the phase brings a new and valued information which greatly expands the potentialities of the SAR. The main products of InSAR include the Digital Elevation Models; the Coherence Maps, employed in land-use classification, and the retrieval of geophysical and biophysical parameters; and the Displacement Maps used to monitor landslides, subsidence areas, etc..

Among the Remote Sensing techniques to generate DEMs, InSAR can play an important role either from the operational point of view (it permits continuous day/night operation and all-weather imaging) or from the economical one. Notwithstanding this potential role, up to day InSAR has not been yet widely employed to generate DEMs; many efforts have to be made in order to establish a correct methodology and to analyse its advantages and limits. This paper would like to be a contribution to these purposes.

2. InSAR Procedure

Although the investigations about the generation of DEMs by means of SAR interferometry started more than a decade ago, up to day a fully automatic and reliable InSAR procedure is not available.

A general InSAR procedure includes the following steps:

1) the acquisition of an interferometric image pair;
2) the precise image registration;
3) the calculation and filtering of the interferogram;
4) the phase unwrapping;
5) the transformation from phases to heights and the geocoding of the DEM.

Among the steps which are critical to the DEM generation are step 4) (unwrapping) and step 5) (transformation and geocoding). Without any doubt, the phase unwrapping problem remains in SAR interferometry the most complex one and a large number of research groups are working on it. The transformation from phases to heights and the geocoding have been very often disregarded, but they are actually very important to get the final product (a geocoded regular grid of 3D points) and hence to assess its quality.

The following paragraphs concern the entire InSAR procedure implemented at DIIAR, giving special emphasis to the original authors' contribution to the latter mentioned step 5).

2.1 Acquisition of an InSAR image pair

The InSAR DEM generation is based on the processing of at least two complex SAR images covering the same area (the complex images contain, for each pixel, amplitude and phase of the radar signal). In order to be used in interferometric way, those images have to be taken from slightly different points of view and have to fulfil two basic conditions.

The first one is related to the so-called "temporal decorrelation" of the images. The information about the three-dimensional (3D) nature of the terrain is closely related to the pixel wise phase difference between the two images. The phase difference (interferometric phase) depends on the time propagation difference between the two signals (in the path satellite- pixel footprint on the ground -satellite) and on the differences on the nature and geometry of the terrain scatterers occurred between the two takes. Since the image pair comes from repeated passes over the same area (for ERS-1/2 the typical

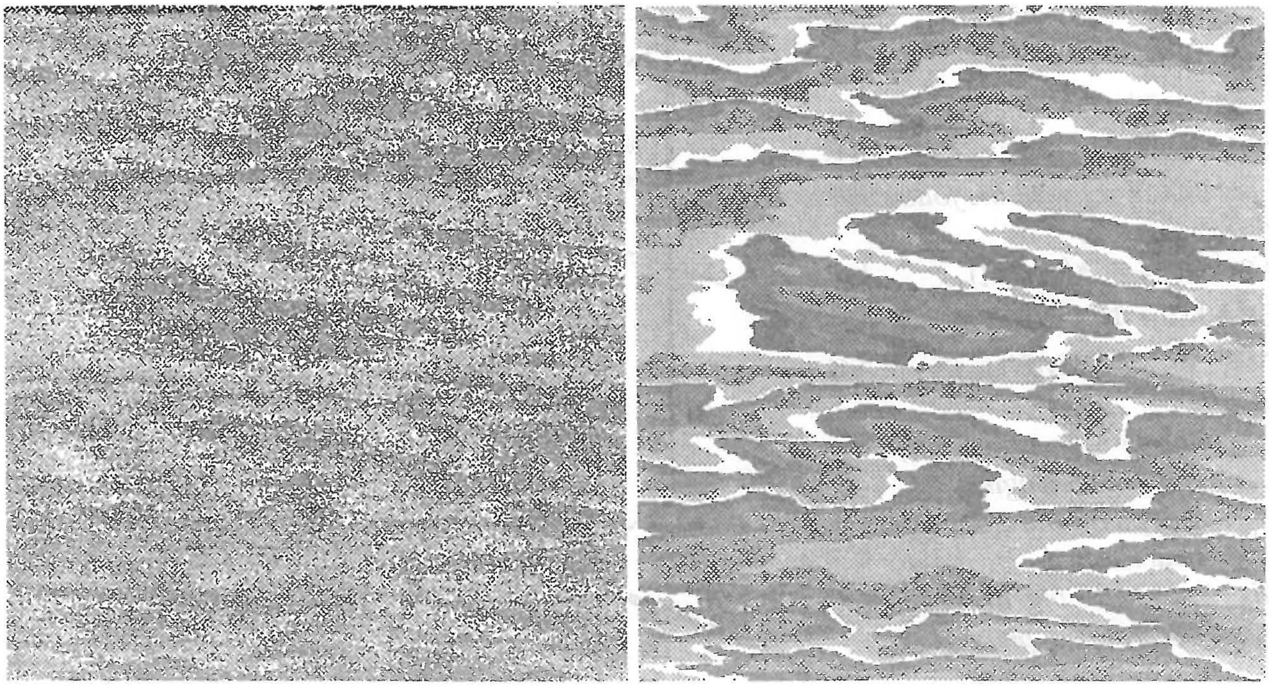

Figure 1: Interferometric phase before and after filtering with the ISAR software.

pass intervals are 1,3,35 and 176 days), and since the useful interferometric information is only related to the time-propagation difference between the two signals, it is very important the physical terrain characteristics do not undergo sensible changes between the different passes.
In case these changes occur (e.g. due to rain, snow or vegetation growth), they originate the "temporal decorrelation" which, depending on its magnitude, can even make the interferometric phase useless for the DEM generation. The second condition to be fulfilled concerns the "geometric decorrelation". The simple fact that the images are taken from not exactly the same point of view engenders a loss of correlation (also called coherence) between the two images and hence noise in the interferometric phase. The image coherence loss is proportional to the satellite baseline length; the "critical baseline" is the value of the base length to which corresponds zero coherence. For ERS-1/2 this value is approximately equal to 1 km, but usually with baselines longer than 500 m there is no more interferometric information because other noise sources sum up to the geometric decorrelation. This limit on the baseline has to be considered in the image pair choice.

2.2 Precise image registration

The key aspect of InSAR lies in the pixel wise phase comparison between the two SAR images. In order to compare the phases, the images must be precisely registered, i.e. pixels with the same co-ordinates in the two images have to correspond to the same footprint on the ground. This condition is not fulfilled by the original images because they only approximately cover the same area and they have been acquired from different points of view and from not exactly parallel orbits.
To perform the registration, the transformation from one image geometry to another must be found, and the resampling of one of the two images must be performed. This operation has to be very precise (realised with sub-pixel accuracy) in order to preserve the interferometric phase quality [Bamler, Just 1993]. Many approaches have been proposed for InSAR registration. In the software ISAR-Interferometric Generator (developed at Polytechnic of Milan and distributed, free of charges, by ESA - European Space Agency), used by the authors, this step is accomplished using both the cross-correlation of the amplitude images (coarse registration) and the amplitude of the local complex coherence (fine registration) [Prati et al. 1994].

2.3 Interferogram calculation and filtering

Once the images are correctly registered, the interferogram is calculated by multiplying an image times the complex conjugate of the other one. The interferogram is a complex image; its phase equals the phase difference between the two images. As each phase, in the original images, is related to the antenna-footprint distance, the interferogram phase is related to the difference of the two distances (antenna1-footprint and antenna2-footprint) and brings the information useful to derive the DEMs.

$-$*Find* S *so that:*

$$\overline{SM} \cdot \overline{V}_M = -\lambda * SM * f_D/2 \quad (1)$$

$-$*Find* P(X,Y,Z) *with the following three equations:*

$$MP = R_0 + \delta_R * (col - 1) \quad (2)$$

$$SP = MP + \Phi_u * \lambda/(4 * \pi) \quad (3)$$

$$\overline{MP} \cdot \overline{V}_M = -\lambda * MP * f_D/2 \quad (4)$$

where:

V_M *master velocity vector,*
λ *radar wavelength,*
f_D *Doppler centroid frequency,*
R_0 *near range,*
δ_R *pixel spacing in range,*
Φ_u *unwrapped phase.*

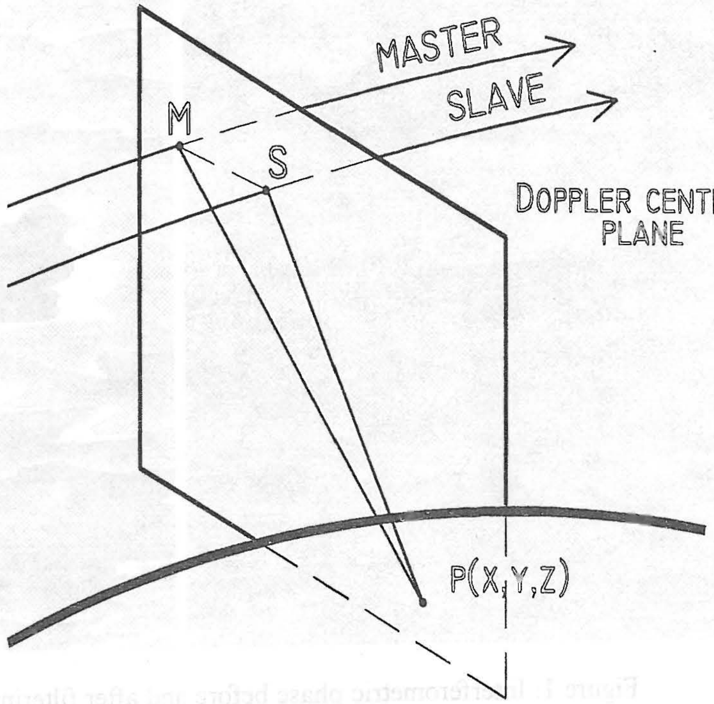

Figure 2: Point wise generation of the 3D irregular grid.

The interferometric phase is corrupted by noise of different kind: thermal noise, noise due to the processing (image focusing, image registration), noise due to geometric and temporal decorrelation, etc..
Usually some filtering is applied to the interferogram in order to reduce the phase noise. The software ISAR (used by the authors to perform this step) allows to eliminate the noise due to geometric decorrelation and partially the one due to the temporal decorrelation (for a detailed description see [Prati et al. 1994]). In Figure 1 an example of interferometric phase before and after filtering is shown; comparing the two images, the improvement of the definition of phase discontinuities (called fringes and discussed in the next section) is evident.

2.4 Phase unwrapping

As mentioned in the previous section, the interferometric phase shows many discontinuities which originate the classical fringe pattern. The fringes are due to the fact that instead of the full phase value ϕ, only the principal value ϕ_p (with $-\pi < \phi_p < \pi$) is known. In order to derive DEMs, it is necessary to obtain the full value ϕ from its principal value ϕ_p (called wrapped phase); this is the task of the phase unwrapping. This operation consists basically of an ambiguity resolution: for each pixel, the integer number of 2π to be added to the principal value must be determined. Many unwrapping approaches have been proposed; the most popular is the so-called "ghost-line" approach [Goldstein, Zebker 1988]. It is based on the assumption that no phase differences greater than π occur between adjacent pixels, (i.e. it is always $\Delta\phi < \pi$); the unwrapping is obtained by integration, pixel by pixel, of the phase differences along a path that does not cross lines of aliasing (called "ghost-lines"). This method, adopted in the authors' procedure, works quite well with interferometric phases of good quality (i.e. with high coherence); on the contrary, dealing with low coherence interferograms, it finds many problems to correctly locate all the "ghost-lines" and often requires a very time-consuming manual editing of the unwrapped phase. Anyway, although it was proposed as a full-automatic procedure, this kind of unwrapping always requires the human operator supervision (i.e. it is a semi-automatic procedure).

2.5 Generation of the DEM

The last step of the procedure is performed using the unwrapped phases, the orbital parameters of the two images and few other sensor parameters (available in the image auxiliary data) describing the imaging geometry. The transformation from unwrapped phases to heights is realised by the authors with a very simple procedure that works point wise and generates an irregular grid of 3D points (i.e. already geocoded). This procedure differs from those usually applied to InSAR, based on approximate transformations from phases to heights, followed by a geocoding (transformation from image space to object space).

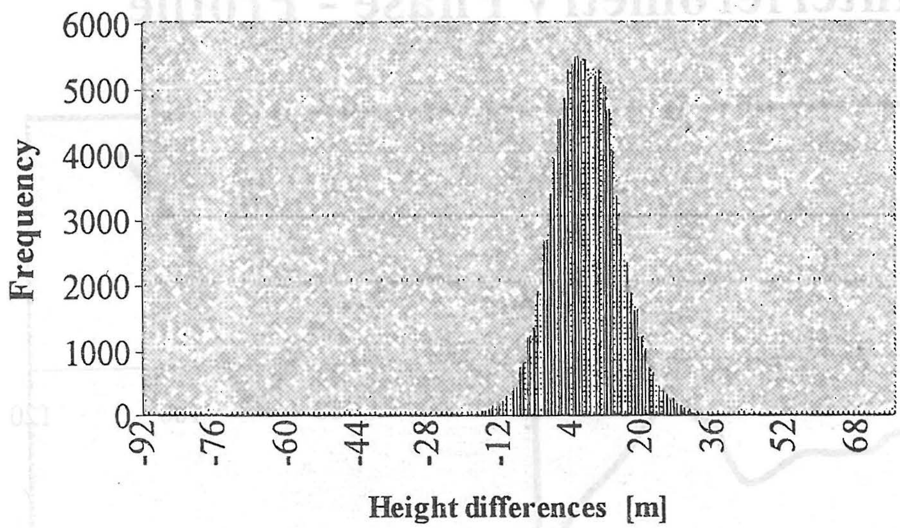

Figure 3: InSAR DEM versus reference DEM - Diagram of the height differences.

Very often this geocoding is similar to those used for the amplitude SAR images, i.e. it requires a known DEM! The proposed procedure does not require any a priori known DEM and, as discussed later, it is quite flexible to allow the fusion of data coming from different sources (e.g. ascending and descending SAR, SAR and SPOT).
For each pixel of the interferogram (i.e. for each unwrapped interferometric phase), once the orbits and the azimuth co-ordinates in the two images are known (the master one has the same geometry of the interferogram, the slave azimuth can be easily derived from the transformation used for the fine registration), the positions and velocities of the master M and slave S satellites are calculated (see Figure 2). Assuming the master M, the slave S and the unknown point P lie in the same plane (the Doppler centroid plane or antenna mid-plane that goes through M), the position of S that fulfil the equation (1) is found. Then, using the range equation (2), the interferometric equation (3) and the Doppler centroid equation (4) the position (X,Y,Z) of the point P is estimated.
In order to generate a good geocoded DEM, both image orbits and sensor parameters have to be precisely determined. Very precise orbits can be acquired through specialised companies (for instance, the ERS-1/2 precise orbits are a standard ESA product). Sensor parameters (and, if necessary, the orbits) can be refined using ground control points (GCPs) visible in the amplitude images; usually a limited number of GCPs (e.g. 8-10 points for one 50x50 km^2 scene) is enough for this purpose.
Repeating the procedure for all the pixels of the unwrapped interferogram, an irregular grid of 3D points is generated. The points are known in a geocentric Cartesian system (the same used for the orbits), thus a transformation to a cartographic projection and to orthometric heights is performed.
The 3D grid generated with the full resolution SAR images has an average spacing of 5 m in the direction parallel to the satellite track and 20 m in the orthogonal direction. Finally does the resampling to get the final regular geocoded grid follow.

3. Analysis of the first results

The authors are involved in an European Union Concerted-Action called ORFEAS (Optical-Radar sensor Fusion for Environmental ApplicationS), including several European research groups (University of Thessaloniki, Cartographic Institute of Catalunya, ETH Zurich, Technical University of Graz, Polytechnic of Milan). An interesting data set, covering south Catalunya-Spain, (ascending and descending ERS-1 SAR images, SPOT images, orthophotos, reference DTM, land-use map, etc.), is available for ORFEAS participants.
The first DEM generated with the above described procedure has been obtained through the ORFEAS data set.
Two ascending ERS-1 sub-images with a baseline length of about 160 m (600 pixels in range by 2700 pixels in azimuth) have been processed using the ISAR software. The mean coherence over the entire intereferogram equals 0.50 before and 0.69 after filtering (i.e. the interferometric phase quality is globally very good!).
In order to obtain a good unwrapped phase over the entire interferogram, a manual editing of the unwrapping program output has been performed. The editing has basically been concerned with the addition of $\pm 2n\pi$ to the phases of the aliasing region situated in proximity of the "ghost lines" (with this satellite

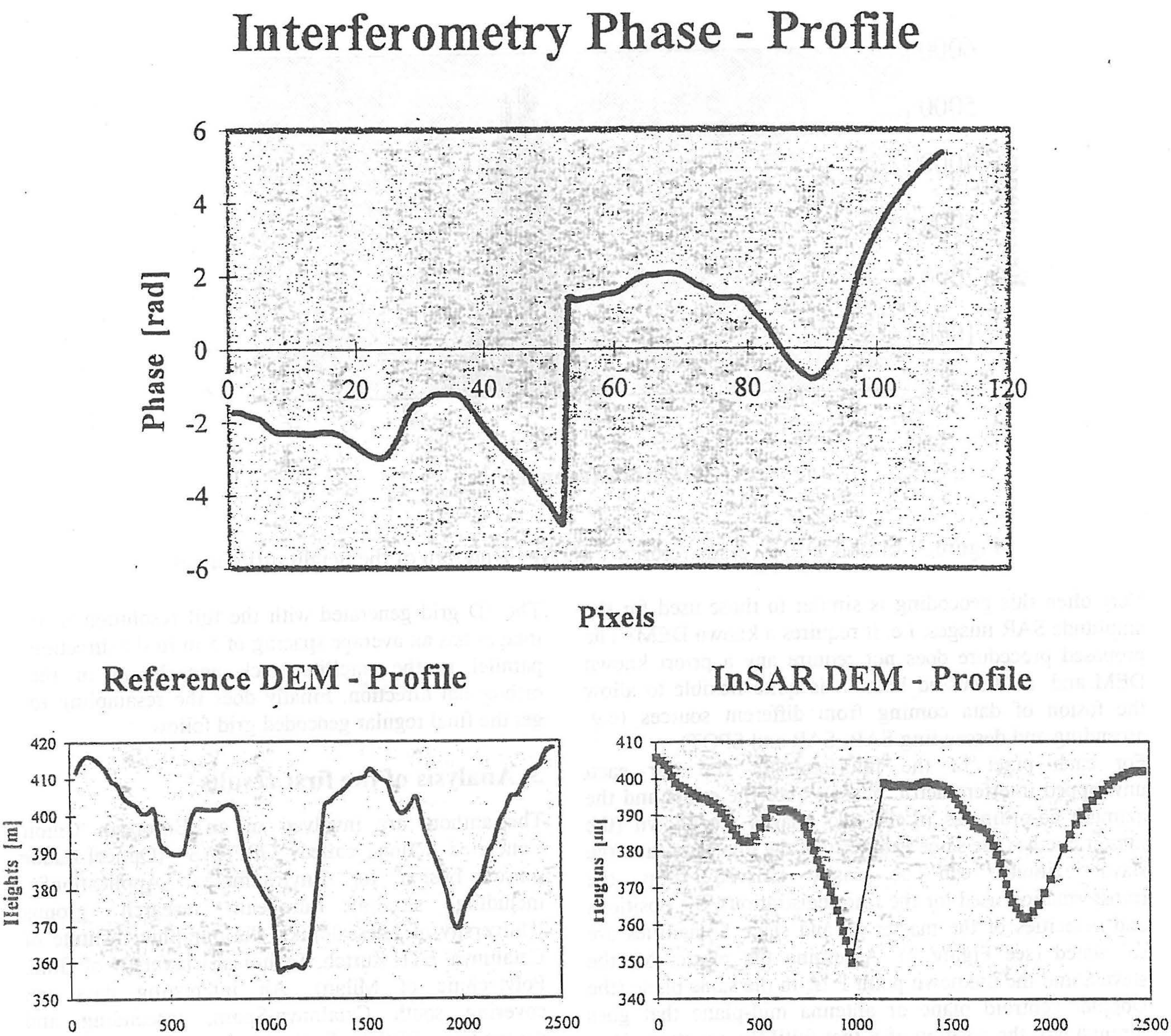

Figure 4: InSAR foreshortening effect.

configuration, a phase wrapping period of 2π corresponds to a terrain drop of about 55m).
Using the precise orbits and the geometry parameters (the near range, the pixel spacing in range and the doppler centroid frequency) refined using 8 GCPs distributed over the entire scene, an irregular grid covering approximately 10x10 km^2 has been generated.
The resampled regular grid with 25 meter spacing has been compared with a reference DEM (coming from photogrammetry), obtaining a RMS error of 9.2 m. In Figure 3, the diagram of the height differences between the two DEMs is shown.

The differences include some peaks (of about 70-90 m) very localised and due to phase unwrapping related errors; these errors usually concern the location of the "ghost-lines".
The obtained accuracy is quite satisfactory; this is certainly due to the very high coherence (i.e. the very good phase quality) and to the gentle terrain variations within the covered area (the maximal height difference in the area is approximately 230m).
The processing time to get the final regular grid can be divided into two parts: the data preparation (e.g. format change, reference system transformation, etc.) and the unwrapping manual editing, which require the support of a human operator - while all the other

operations, though needing several hours of processing time (about 5-6 hours with a Pentium-100 MHz for a 10x10 km^2 area and a 1.5 million grid points), are performed in an automatic way.

4. Data fusion potentiality

The InSAR technique can generate DEM of good quality (i.e. good accuracy), assumed at least a medium-high coherence (e.g. > 0.5) over the entire interferogram and gentle terrain variations within the covered area. Dealing with more complex topography many problems arise. In fact, the slant range nature of the SAR data implies big distortion effects when mountainous and hilly terrain is imaged [Schreier 1993]. The first effect is called Foreshortening: the front slopes of mountains are shortened, i.e. appear compressed in the images. The reason of this compression can be easily understood in the extreme case when the slope's elevation angle equals the radar beam off-nadir angle (i.e. the local incidence angle equals 90 degrees): all the points of the slope lie at the same slant range distance to the antenna so, even a few kilometre long side is imaged in only one pixel. The same applies to less inclined slopes but with a mitigated compression effect. An extreme case of foreshortening is Layover in which the top of a hill is nearer to the antenna than the bottom of the hill. Subsequently, the hill top is imaged early than the bottom, thus inverting the local mountain geometry. The last effect (called Shadow) occurs on hill slopes, which are bent away from the look direction. If the slope is steeper than the incidence of the radar beam, the terrain is not seen by the radar (so no information about the slope is available). The geometric distortions represent an inner limitation of the SAR system that affects both classical and interferometric applications.

A good example of foreshortening effect is shown in Figure 4. The interferometry unwrapped phase profile along the slant range presents a jump of about 2π; analysing the phase field in the area around (operation done during the phase manual editing), no phase unwrapping related errors can be found; the only possible explanation is the foreshortening effect. Actually, the corresponding profile of the generated DEM (the square dots represent the generated 3D points) presents a height jump of about 55m with no points in all the front slope compressed in the SAR images. The InSAR generated profile (see Figure 4) copes quite good with the reference one, but this occurs because the compressed slope has a limited length (less than 200 m). Dealing with bigger slopes, the generated grid will present big holes in correspondence to the compressed slopes (i.e. the final DEM accuracy is deteriorated).

In order to improve the quality of the DEMs in mountainous regions, the fusion of data coming from different sources could show good potentialities. The foreshortening affects only the front slopes of the mountains, thus the DEM accuracy can be improved by combination of ascending and descending passes over the same area. Also optical data (e.g. the 3D points generated with SPOT stereo images) can be combined with InSAR data. The InSAR procedure explained in paragraph 2.5 is quite flexible to allow this data fusion. Each source of data (e.g. ascending SAR pair, descending SAR pair, SPOT stereo pair) can be separately processed to generate different set of 3D points (in the same reference system); a quality factor (e.g. the height variance) can be assigned to each point. The quality factor can be a function of the local coherence for InSAR points and a function of the local image correlation for SPOT points. All the points, with the relative weights, can be used to estimate the final DEM (with an estimation procedure that takes into account the point weights). The effectiveness of the data fusion will be proved using the above mentioned ORFEAS data set.

5. Conclusions

The first results obtained processing a SAR image pair covering South Catalunya with the InSAR procedure implemented at DIIAR are quite satisfactory. The proposed procedure does not require any a priori known DEM and it is quite flexible to allow the fusion of data coming from different sources (e.g. ascending and descending SAR, SAR and SPOT). The future work at DIIAR will concern the study of the integration and fusion potentialities of optical and radar data using the ORFEAS data set.

6. References

Bamler R., Just D., 1993. Phase Statistics and Decorrelation in SAR Interferometry. Proceedings of IEEE-IGARSS '93, Tokyo, August 1993, pp. 980-984.

Goldstein R.M., Zebker H.A., 1988. Satellite Radar Interferometry: Two-dimensional Phase Unwrapping. Radio Science, vol.23, No. 4, pp.713-720.

Prati C., Rocca F., Monti Guarnieri A., Pasquali P., 1994. ERS-1 SAR Interferometric Techniques and Applications. ESA Report No. 3-7439/92/HGE-I.

Koskinen J., 1995. The ISAR-Interferogram Generator Manual ESA/ESRIN, Frascati, Italy.

Schreier G., 1993. SAR Geocoding: Data and Systems. Wichmann Verlag, Karlsruhe - Germany.